

Organic & Biomolecular Chemistry

www.rsc.org/obc

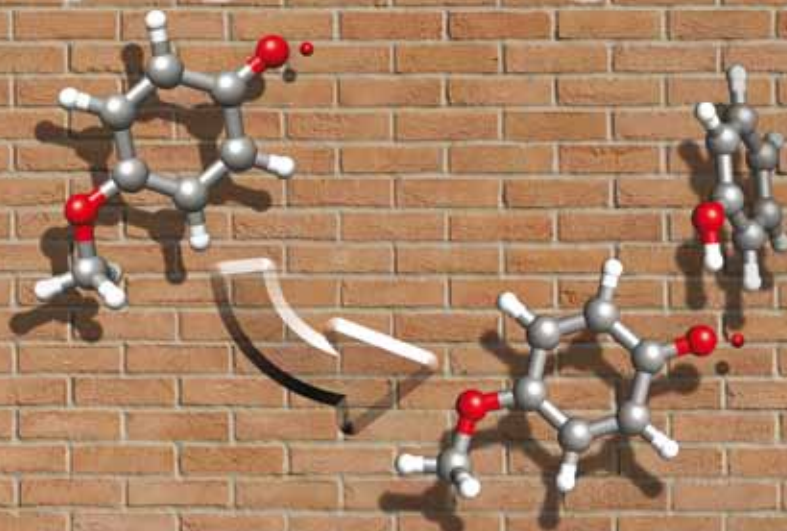
Volume 8 | Number 14 | 21 July 2010 | Pages 3085–3344

Downloaded on 17 August 2010
 Published on 17 May 2010 on http://pubs.rsc.org | doi:10.1039/C003302B

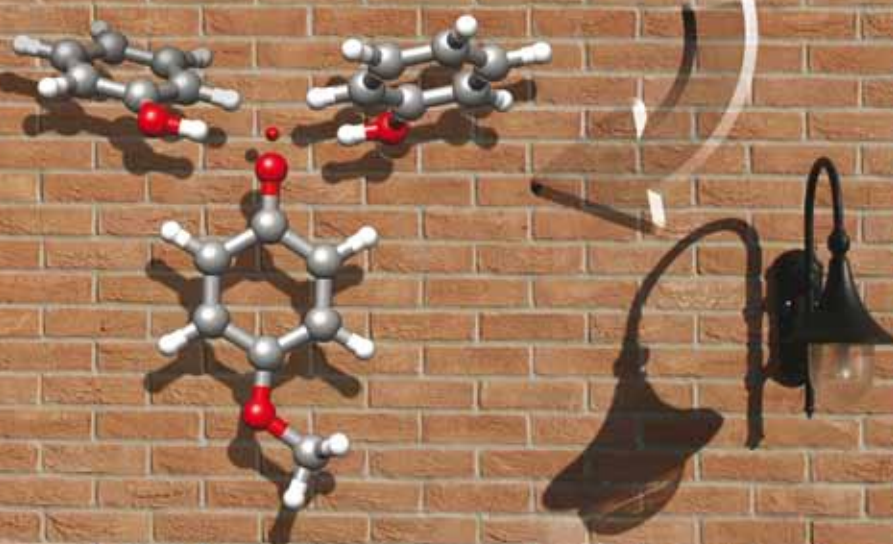


ESR Spectroscopy

Hydrogen-bonding effects



DFT Calculations



ISSN 1477-0520

RSC Publishing

FULL PAPER

Riccardo Amorati *et al.*
 Hydrogen hyperfine splitting constants for phenoxyl radicals by DFT methods: regression analysis unravels hydrogen bonding effects

FULL PAPER

Stefan Bräse *et al.*
 Enantioselective total synthesis of plakotenin, a cytotoxic metabolite from *Plakortis sp*

Hydrogen hyperfine splitting constants for phenoxyl radicals by DFT methods: regression analysis unravels hydrogen bonding effects†

Riccardo Amorati,^{*a} Gian Franco Pedulli^a and Maurizio Guerra^b

Received 19th February 2010, Accepted 20th April 2010

First published as an Advance Article on the web 17th May 2010

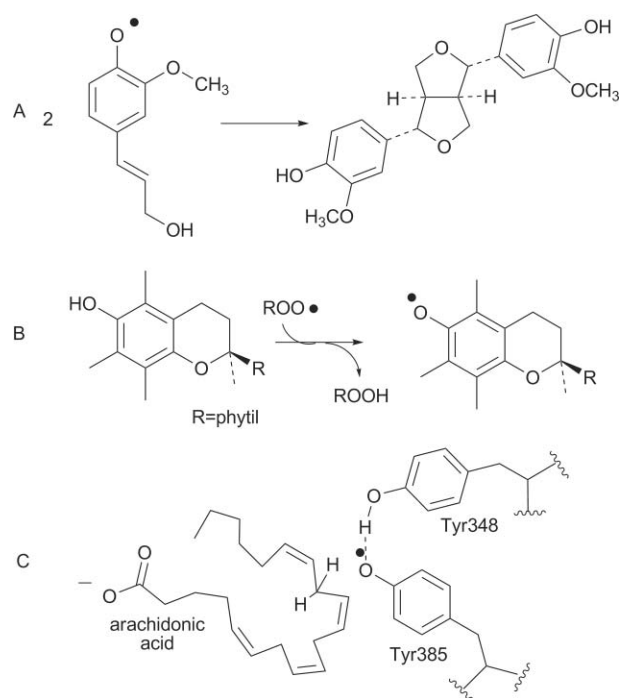
DOI: 10.1039/c003302b

DFT calculations using the B3LYP functional, medium-sized basis sets and empirical scaling of the results provide quantitative estimates of the hydrogen isotropic hyperfine splitting constants (*hscs*) in 2,6-di-alkyl phenoxyl radicals (1–11). Literature *hscs* for phenoxyl (12), 4-methylphenoxyl (13) and 4-methoxyphenoxyl (14) radicals, on the other hand, are poorly predicted by using this method. This different behaviour is explained considering that experimental *hscs* of 12–14 are influenced by H-bonds formed between phenoxyls and their parent phenols, usually present in large amounts in solution as radical precursors. This was confirmed experimentally by measuring the EPR spectra of 12–14 in the presence of increasing amounts of their parent phenols, and by calculating the *hscs* in the case of the formation of 1 : 1 and 1 : 2 complexes between these radicals and phenol. Relevance of these results to the choice of reference *hscs* as benchmarks for theoretical calculations and to kinetic and thermochemical determinations on unhindered phenoxyl radicals is discussed.

Introduction

Phenoxyl radicals represent one of the most important families of biologically relevant radicals. Their formation is fundamental in enzyme catalysis,¹ in photosynthetic events,² in the biosynthesis of lignanes³ and in the action of phenolic antioxidants⁴ (Scheme 1). Most information about phenoxyl radicals is provided by electron paramagnetic resonance (EPR) spectroscopy, which allows to detect and characterize structural and dynamic properties of radicals in a wide range of environments.⁵ Isotropic hyperfine splitting constants (*hscs*),‡ measured in the case of fast rotational motion of radicals, give valuable insight into electronic properties and presence of intra and inter-molecular hydrogen bonding interactions. For instance, the addition of hexafluoropropanol (HFP), a strong H-bond donor, has dramatic effects on isotropic *hscs* of several phenoxyl radicals, including α -tocopheroxyl,⁶ while H-bond accepting solvents, such as dimethylsulfoxide and acetonitrile, cause noticeable changes on *hscs* in neutral semiquinones.⁷

The abundance of data that can be extracted from experimental *hscs* is nowadays interpreted with the help of theoretical calculations. Among the various approaches, methods relying on density functional theory represent a convenient compromise between accuracy and computational cost.⁵ The ability of DFT methods to reproduce hydrogen *hscs* in the phenoxyl radical in vacuum or



Scheme 1 Relevant examples of phenoxyl radicals involved in biological processes. A: biosynthesis of the lignan (+)-pinoresinol;³ B: antioxidant action of α -tocopherol;^{4a} C: tyrosyl radical in the active site of prostaglandin H synthase (PGHS-1).^{1c}

in aqueous environment has been already investigated in the past. Eriksson noticed that hybrid DFT calculations provide reasonably good estimates of hydrogen *hscs* in π radicals, such as phenoxyl and benzyl.⁸ The hyperfine splitting constants for the phenoxyl radical were also calculated by Barone and co-workers using the B3LYP functional and the basis sets EPR-II and EPR-III.⁹ By using the PCM model, the *hscs* for the *ortho*, *meta* and *para* hydrogens were computed to change from 7.3, 2.8, 9.4 G in the gas phase

^aDepartment of Organic Chemistry "A. Mangini", University of Bologna, Via S. Giacomo 11, 40126, Bologna, Italy. E-mail: riccardo.amorati@unibo.it; Fax: (+39) 051-209-5684

^bISOF, Consiglio Nazionale delle Ricerche, Via P. Gobetti 101, 40129, Bologna, Italy

† Electronic supplementary information (ESI) available: Experimental *hscs* from literature for 1–14; experimental *hsc* and EPR spectra at every parent phenol concentration for 12–14; plots of experimental *versus* calculated *hsc* for each computational level. See DOI: 10.1039/c003302b

‡ Theoretical calculations provide hyperfine coupling constants, which can be positive or negative at a given atom. Hyperfine splitting constants, measurable from EPR spectra, are the absolute values of the corresponding coupling constants.

to 6.6, 2.4, 9.8 G in water⁹ (experimental values in H₂O: 6.6, 1.9, 10.2 G).¹⁰ Similar results were also obtained by Chipman, who investigated the effect of water by employing the B3LYP functional and a purposely tailored basis set ([631|41]), and by explicitly considering H₂O molecules.¹¹

Validation of theoretical methods for the description of a molecular property critically depends, however, on the availability of good-quality experimental values. While all *hscs* for phenoxyl radicals reported in literature are coincident when measured in water,¹⁰ those measured in apolar solvents are not. The *hscs* for the phenoxyl radical generated in CCl₄ using photolysis and a flow system are 7.02, 2.05 and 10.13 G for *ortho*, *meta* and *para* hydrogens,¹² while the *hscs* obtained by stationary photolysis in benzene^{13,14} are, on the basis of the considerations made above, unexpectedly similar to those measured in water: 6.57, 1.84 and 10.07 G for *ortho*, *meta* and *para* hydrogens, respectively.¹³

In this work, we show that relatively inexpensive DFT methods predict, in some cases almost quantitatively, hydrogen *hscs* of phenoxyl radicals, and provide an explanation for the less clear aspects of the chemistry of these radicals.

Experimental section

Materials

Solvents, phenol, 4-methylphenol and 4-methoxyphenol were of the highest grade commercially available and were used as received. Di-*tert*-butylperoxide was percolated through activated basic alumina and stored at 5 °C.

EPR experiments

Deoxygenated benzene solutions containing the investigated phenol ($5 \times 10^{-4} - 2$ M) and di-*tert*-butylperoxide (5% v/v) were sealed under nitrogen in a suprasil quartz EPR tube. The sample was inserted in the cavity of an EPR spectrometer and photolyzed with the unfiltered light from a 500 W high-pressure mercury lamp. Hyperfine splitting constants were determined by numerical fitting of experimental spectra¹³ and the error is within ± 0.02 G.

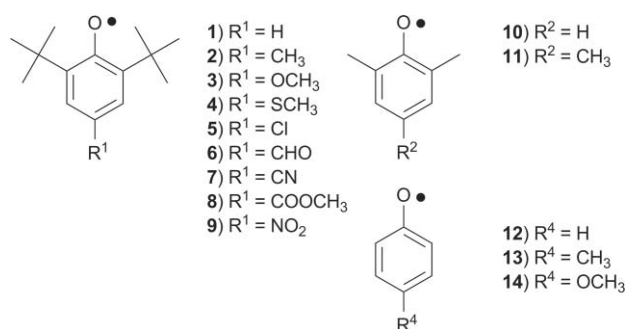
Computational details

DFT calculations were carried out using the Gaussian03 system of programs.¹⁵ Geometries were optimized at the B3LYP/6-31G(d) level. This level has been demonstrated to yield sufficiently accurate structures for phenoxyl radicals.⁹ Enthalpies at 298 K were computed at the stationary points from frequency calculations using a scaling factor of 0.9806 to account for anharmonicity.¹⁶ The nature of the ground states was verified by frequency calculations (zero imaginary frequency). *Hscs* were obtained from the absolute values of coupling constants calculated by using the functionals B3LYP¹⁷ and PBE0¹⁸ (in Gaussian03: PBE1PBE). Different basis sets were used: 6-31G(d),¹⁹ 6-31+G(d,p),²⁰ 6-311+G(2df,p) which has been previously suggested for reliable *hsc* calculations,²¹ and the EPR-III basis set.²² The tight SCF convergence criteria was used in single point calculations. The influence of vibrational averaging on coupling constants was not investigated, as it was previously found to have negligible effect in this kind of radicals.⁹

Results and discussion

Considering the difficulty of calculating “exact” *hscs* from a single calculation,⁵ in the present work we used empirical relationships between calculated and experimental constants to obtain reliable *hscs* at a low computational cost. This approach is based on the fact that, even at low levels of theory, the linearity of the experimental *vs.* calculated *hscs* for a wide range of radicals is excellent.²³

To compare calculated *hscs* with homogeneous experimental data, only *hscs* measured in benzene were chosen from the literature. Typically, these data were obtained by stationary photolysis of the parent phenols, in the presence of small amounts of *tert*-butyl peroxide.^{13,24,25} The experimental values used to validate the computational approach are reported in ESI.† Very small *hscs*, that are those given by the hydrogens of the *tert*-butyl groups and of the *para* substituents of **6** and **8** (Scheme 2), were not included in the regression analysis.



Scheme 2

1. Regression analysis of *hscs* of hindered phenols

Good straight lines are obtained when the experimental *hscs* of radicals **1–11** are plotted *versus* the calculated ones (see Fig. 1 and ESI†). Their slope, intercept and correlation coefficients are reported in Table 1. Both B3LYP and PBE0 functionals provide, after scaling, *hscs* in good agreement with experiments, B3LYP being somewhat superior when all *hscs* are considered. These results also confirm that good correlations between experimental and calculated *hscs* are achieved already with small basis sets,²³ such as 6-31G(d), with the exception of radical **4** which requires the 6-311+(2df,p) basis set to be properly simulated (see ESI†).

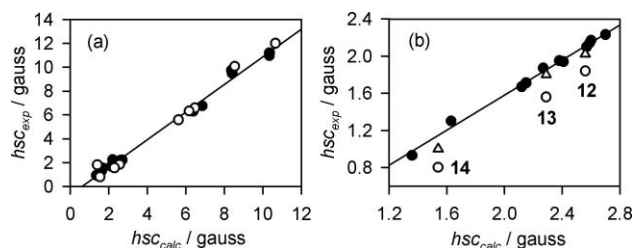


Fig. 1 Experimental *versus* calculated hyperfine splitting constants for **1–11** (●)^{13,24,25} and for **12–14** (○: literature values;^{6,13} △: from this work, at low parent phenol concentration). Panel a: all *hscs*. Panel b, *hscs* for *meta* hydrogens.

Table 1 Experimental versus calculated hyperfine splitting constants: data analysis^a for phenoxy radicals **1–11** (in gauss)

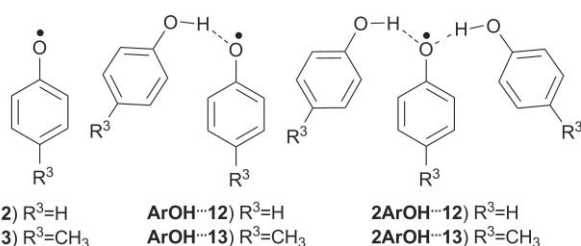
	B3LYP			EPR-III ^b	PBE0	
	6-31G(d)	6-31+G(d,p)	6-311+G(2df,p)		6-311+G(2df,p)	EPR-III ^b
All H						
Slope	1.152	1.140	1.160	1.070	1.179	1.127
Intercept	-1.123	-0.964	-0.728	-0.680	-1.551	-1.788
r ²	0.988	0.993	0.993	0.994	0.979	0.985
meta H						
Slope	0.863	0.850	0.943	0.894	0.778	0.742
Intercept	-0.512	-0.348	-0.306	-0.379	-0.587	-0.671
r ²	0.990	0.993	0.993	0.998	0.993	0.998

^a $H_{sc,exp} = \text{slope} \times h_{sc,calc} + \text{intercept}$. ^b Excluding radicals from compounds **4** and **5** since the basis sets for S and Cl atoms are lacking in EPR-III.

2. Experimental determination and simulation of *hscs* of unhindered phenols

A peculiar behaviour is observed when plotting in the same graph experimental vs. calculated *hscs* of *ortho* unhindered radicals **12–14** and those of **1–11** (Fig. 1). Phenoxy radicals **12–14** are more or less on the same line of the hindered ones, if considering all *hscs* (Fig. 1a), but when restricting the analysis only to the *meta* hydrogens, they are visibly outside the main regression line (Fig. 1b, empty circles). The *hscs* for **12–14** are still outside the regression line also employing the PBE0 functional or different basis sets (see ESI†). This suggests that the problem may not be in the method used to calculate *hscs*, but in experimental data. As it has been previously reported that *hscs* are strongly influenced by formation of H-bonds with HFP,⁶ we hypothesized that parent phenols present in the samples as precursors of phenoxy radicals might behave as H-bond donors. These interactions are absent in the case of **1–11** as the ability to donate H-bond is drastically reduced by steric repulsion.^{26,27,§}

To check this hypothesis, we measured the EPR spectra of radicals **12–14** by stationary photolysis at various concentrations of their respective parent phenols (Fig. 2). Experimental data, summarized in Fig. 2, show remarkable changes of *hscs* with the concentration of the parent phenols. The measured overall *hscs* are expected to be due to the *hsc* of each species present in solution (see Scheme 3 for the most important ones), weighted for their molar fractions, as H-bonding equilibria are fast in the time scale of EPR.⁶ *Hscs* measured at the smallest concentration of the parent phenols provide an estimate of the “true” *hscs* in benzene (Table 2) and are in better agreement with calculated ones than those reported in literature (Fig. 1b, triangles).



Scheme 3 Complexes formed by radicals **12** and **13** and their parent phenols.

§ The H-bond donating ability, expressed by the α_2^H parameter, of phenol, 4-methylphenol, 4-methoxyphenol, 2,6-*t*Bu-4-MeC₆H₂OH and HFP are 0.60, 0.57, 0.57, ≈0.18, 0.77 respectively (ref.26,27,28).

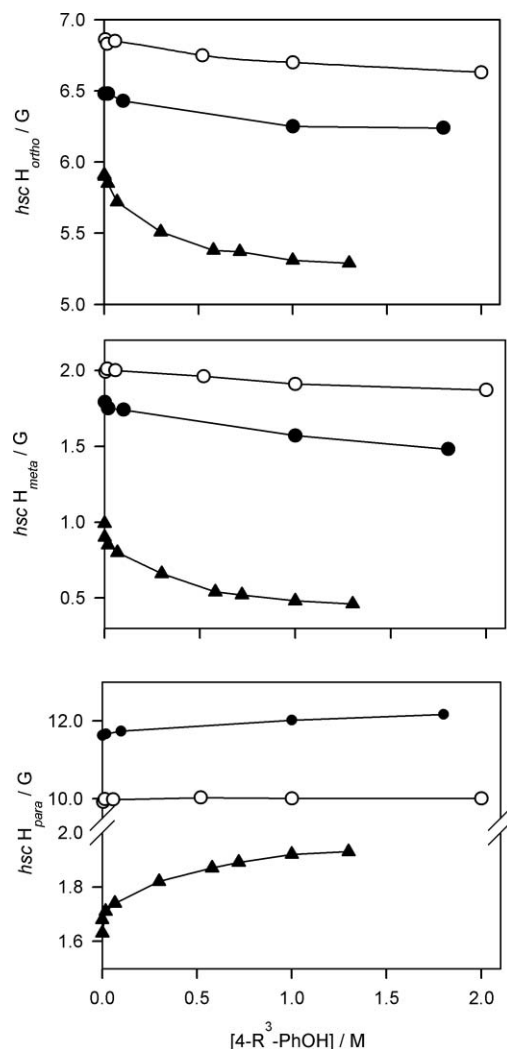


Fig. 2 Proton hyperfine splittings measured in the EPR spectra of radicals **12** (○), **13** (●) and **14** (▲) obtained by photolyzing increasing amounts of phenol (R³=H), 4-methylphenol (R³=CH₃) and 4-methoxyphenol (R³=OCH₃) in benzene containing 10% of ^tBuOO^tBu.

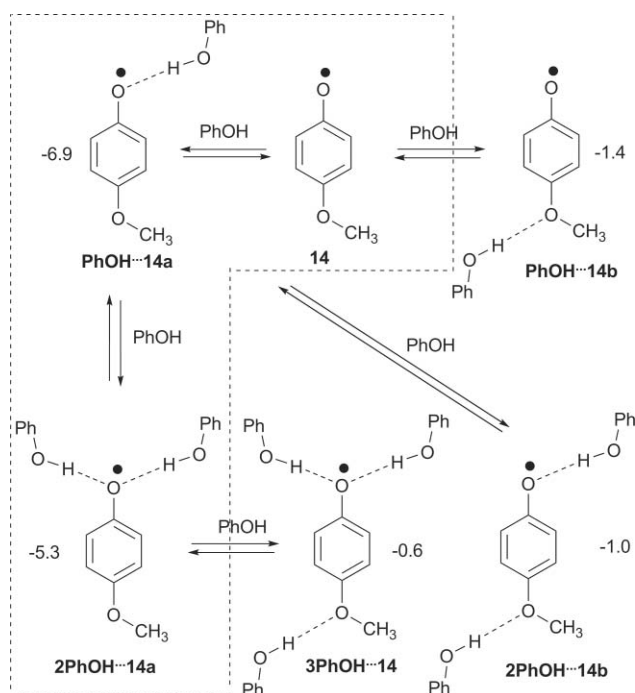
To have further insight into H-bonding effect on the *hscs* of unhindered phenoxy radicals, we investigated radicals **12–14** by DFT calculations in the presence of their parent phenols. The geometries of the H-bond complexes, shown in Scheme 3 for **12** and **13**, were optimized at the B3LYP/6-31G(d) level. Phenol was

Table 2 Comparison between the hsc values (in gauss) for radicals **12–14** calculated in the absence and in the presence of H-bond interactions with one or two phenol molecules and the experimental hsc s measured at the lowest and at the largest parent phenol concentration

Radical	Hsc 2,6 (2H)		Hsc 3,5 (2H)		Hsc 4	
	Calc ^a	Exp	Calc ^a	Exp	Calc ^a	Exp
12	6.78	6.86 ^b	2.11	2.01 ^b	9.18	9.92 (H) ^b
PhOH... 12	6.58		1.95		9.25	
2PhOH ... 12	6.35	6.63 ^c	1.81	1.87 ^c	9.39	10.01 ^c
13	6.43	6.48 ^b	1.85	1.79 ^b	11.64	11.63 (CH ₃) ^b
PhOH... 13	6.14		1.64		12.18	12.17 ^c
2PhOH ... 13	5.84	6.24 ^c	1.42	1.48 ^c	12.68	
14	5.79	5.91 ^b	1.15	0.99 ^b	0.91	1.68 (OCH ₃) ^b
PhOH... 14a	5.32		0.79		1.53	
PhOH... 14b	6.07		1.38		0.97	
2PhOH ... 14a	4.85	5.29 ^c	0.46	0.46 ^c	1.74	1.93 ^c
2PhOH ... 14b	5.63		1.06		1.17	
3PhOH ... 14	5.21		0.75		1.35	

^a hsc s were calculated at the B3LYP/6-311+G(2df,p)//B3LYP/6-31G(d) level and then corrected using the following equations taken from Table 1: *ortho* and *para* positions: $hsc_{calc} = 1.16 \times hsc_{calc} - 0.728$; *meta* position: $hsc_{calc} = 0.943 \times hsc_{calc} - 0.306$. ^b Measured in the present work at small concentration of the parent phenol. ^c Measured in the present work at large concentration of the parent phenol.

chosen as H-bond donor in all cases to simplify calculations, considering that phenol, 4-methylphenol and 4-methoxyphenol have approximately the same H-bond donating ability,^{26,27} In the case of **14**, where the situation is complicated by the presence of two H-bond acceptors, *i.e.* the $-O\cdot$ and the $-OCH_3$ groups, the structures reported in Scheme 4 were examined.



Scheme 4 Possible complexes between radical **14** and phenol, and calculated enthalpy for H-bond formation ΔH_f (kcal mol^{-1}). The species preferentially formed are evidenced.

hsc s were calculated at the B3LYP/6-311+G(2df,p)//B3LYP/6-31G(d) level and, to be compared to experimental results, were corrected using the correlation equations for this level of theory (see footnote *a* of Table 2). From the results reported in

Table 2, it can be inferred that calculations correctly reproduce the hsc variation observed experimentally, that is, on increasing the number of H-bond donors (that is, the concentration of the parent phenol), hsc s for the *ortho* and *meta* hydrogens decrease, while the *para* hsc increases.

Quantitative considerations can be made by restricting the analysis only to the *meta* constants. Table 2 shows that the experimental hsc s measured in radicals **12** and **13** at the largest concentrations of the parent phenol (1.8 and 2.0 M respectively) are between the values calculated for the phenoxyl radicals forming one or two H-bond interactions. Therefore, it may be concluded that phenoxyl radicals **12** and **13** are complexed by, on average, between one and two parent phenol molecules.

In the case of **14**, complexation of the two possible H-bond accepting sites (*i.e.* $ArO\cdot$ and OCH_3 moieties) has very different effects on hsc s. H-bond donation to phenoxyl oxygen lowers *meta* hydrogens hsc , whereas interaction with the oxygen atom of the methoxy group has about equal but opposite effect on this constant. The very low value of the *meta*-H hsc determined experimentally at the largest concentration of the parent phenol (1.4 M) is compatible only with the structure **2PhOH**...**14a** (Scheme 4). On the other hand, we can exclude any structure with the OCH_3 group acting as H-bond donor. This result is in good agreement with the expected order of formation of the various complexes, which can be derived from the values of the enthalpy estimated for H-bond formation, reported in Scheme 4.

It may be also noted that **14** is complexed to a larger extent than radicals **12** and **13**, implying that the H-bonds between radical **14** and 4-methoxyphenols are stronger than those formed between radicals **12** and **13** and their parent phenols. This observation was confirmed by calculating the ΔH_f values for the relevant H-bonding equilibria, reported in Table 3.

Conclusions

In this work we have demonstrated that relatively cheap DFT calculations using the popular B3LYP functional and small

Table 3 Calculated (B3LYP/6-311+G(2df,p)//B3LYP/6-31G(d)) strength of the H-bonds between phenoxyl radicals **12–14** and phenol molecules^a

Radical	ΔH_f (PhOH... [•] OAr) ^b	ΔH_f (2PhOH... [•] OAr) ^c
12	−5.8	−4.4
13	−6.2	−4.8
14	−6.9 ^d	−5.3 ^e

^a kcal mol^{−1}, ^b PhOH + [•]OAr = PhOH...[•]OAr, ^c PhOH + PhOH...[•]OAr = 2PhOH...[•]OAr, ^d **PhOH...14a**, ^e **2PhOH...14a**.

and medium-sized basis sets provide, after scaling the results, quantitative estimates of the proton hyperfine splitting constants in phenoxyl radicals. The agreement between experimental and calculated *hscs* is particularly good in the case of the *meta* H-atoms, reasonably because the absence of substituents in this position makes the regression approach more effective. For the other hydrogens, the procedure described herein leads to *hscs* that are ± 0.5 G with respect to experimental values, thus representing a good starting point for spectra interpretation in EPR spectroscopy. This procedure has been successfully applied to clarify the association state of three unhindered phenoxyl radicals.

Our results show that the majority of the *hscs* reported in the literature for unhindered phenoxyl radicals in apolar solvents^{13,14} actually refer to the radicals forming extensive H-bonds with parent phenols molecules. Unfortunately, as unhindered phenols are very good H-bond donors, this can be avoided only by using very diluted solutions, such as those employed in the present work and in the experiments of Graf *et al.*¹² Moreover, little differences in parent phenol concentrations may lead to significant changes in *hscs*, thus explaining why in apolar solvents there is such variability of *hsc* values. In water, where each H-bond accepting or donating site of the investigated phenoxyls is solvated by H₂O molecules, *hscs* are not dependent on the parent phenol concentration and are therefore much more reproducible.¹⁰

This observation also opens several questions about the reliability of kinetic and thermodynamic measures carried out on unhindered phenoxyl radicals in apolar solvents. In the case of the determination of the bond dissociation enthalpy (BDE) of the phenolic O–H *via* the EPR equilibration technique,¹³ or *via* the photoacoustic calorimetric method (PAC),²⁸ usually performed with parent phenols in the 0.05–0.5 M concentration range, error compensations can be envisaged as the cause for the relatively good agreement between measured and computed results. The BDE-lowering effect given by H-bonding with the phenoxyl radicals⁶ are counterbalanced by the BDE-increasing effect of H-bonds formed by the ArOH group in the parent phenol.²⁷

Regarding reactions of formal H-atom abstraction by ArO[•] radicals, such as that one involved during the catalytic cycle of prostaglandin H synthase (see Scheme 1),^{1c} it can be expected that a phenoxyl radical accepting one H-bond from another phenol is still able to give H-atom abstraction. However, since the phenoxyl oxygen atom is a much better acceptor (ArO[•], $\beta_2^H \approx 0.5$)⁶ than the phenolic oxygen atom (PhOH, $\beta_2^H = 0.22$),²⁹ the H-bond stabilizes the reagent radical more than the product phenol, so that the driving force for H-atom abstraction is reduced. Formation of two H-bond interactions, as happens when generating phenoxyl radicals in the presence of very concentrated solutions of the parent phenol,³⁰ may lead to further reactivity decrease. The

increased persistency, that reflects the decrease of the rate of self-decay, of phenoxyl radicals at large HFP concentrations⁶ seems to confirm this hypothesis. Further clarification of these points is of great interest given the presence of ArOH...[•]OAr H-bonded structures in natural systems, such as that shown in Scheme 1.

Finally, it can be also concluded that experimental *hscs* in apolar solvents should be taken with caution as a reference for theoretical calculations, in particular for radicals which are good H-bond acceptors or donors, unless very low concentrations of the precursors have been used in the EPR determinations.

Acknowledgements

Financial support from MIUR (Research projects “Radicals and Radical Ions: Basic Aspects and Role in Chemistry, Biology, and Material and Environmental Sciences”, contract 2006033539) is gratefully acknowledged.

Notes and references

- (a) J. Stubbe and W. A. van der Donk, *Chem. Rev.*, 1998, **98**, 705; (b) J. C. Wilson, G. Wu, A. Tsai and G. J. Gerfen, *J. Am. Chem. Soc.*, 2005, **127**, 1618; (c) A. Tsai and R. J. Kulmacz, *Arch. Biochem. Biophys.*, 2010, **493**, 103.
- C. Carra, N. Iordanova and S. Hammes-Shiffer, *J. Am. Chem. Soc.*, 2003, **125**, 10429.
- L. B. Davin and N. G. Lewis, *Curr. Opin. Biotechnol.*, 2005, **16**, 398.
- (a) G. W. Burton, T. Doba, E. J. Gabe, L. Hughes, F. L. Lee, L. Prasad and K. U. Ingold, *J. Am. Chem. Soc.*, 1985, **107**, 7053; (b) R. Amorati, A. Cavalli, M. G. Fumo, M. Masetti, S. Menichetti, C. Pagliuca, G. F. Pedulli and C. Viglianisi, *Chem.–Eur. J.*, 2007, **13**, 8223.
- R. Improta and V. Barone, *Chem. Rev.*, 2004, **104**, 1231.
- M. Lucarini, V. Mugnaini, G. F. Pedulli and M. Guerra, *J. Am. Chem. Soc.*, 2003, **125**, 8318.
- R. Amorati, P. Franchi and G. F. Pedulli, *Angew. Chem., Int. Ed.*, 2007, **46**, 6336.
- L. A. Eriksson, *Mol. Phys.*, 1997, **91**, 827.
- C. Adamo, R. Subra, A. Di Matteo and V. Barone, *J. Chem. Phys.*, 1998, **109**, 10244.
- P. Neta and R. W. Fessenden, *J. Phys. Chem.*, 1974, **78**, 523; W. T. Dixon and D. Murphy, *J. Chem. Soc., Faraday Trans. 2*, 1977, **73**, 1475.
- D. M. Chipman, *J. Phys. Chem. A*, 2000, **104**, 11816.
- F. Graf, K. Loth and H. H. Gunthard, *Helv. Chim. Acta*, 1977, **60**, 710.
- M. Lucarini, P. Pedrielli, G. F. Pedulli, S. Cabiddu and C. Fattuoni, *J. Org. Chem.*, 1996, **61**, 9259.
- S. A. Weiner, *J. Am. Chem. Soc.*, 1972, **94**, 581.
- M. J. Frisch, G. W. Trucks, H. B. Schlegel, G. E. Scuseria, M. A. Robb, J. R. Cheeseman, J. A. Montgomery, T. Vreven, K. N. Kudin, J. C. Burant, J. M. Millam, S. S. Iyengar, J. Tomasi, V. Barone, B. Mennucci, M. Cossi, G. Scalmani, N. Rega, G. A. Petersson, H. Nakatsuji, M. Hada, M. Ehara, K. Topyota, R. Fukuda, J. Hasegawa, M. Ishida, T. Makajima, Y. Honda, O. Kitao, H. Nakai, M. Klene, X. Li, J. E. Know, H. P. Hratchian, J. B. Cross, V. Bakken, C. Adamo, J. Jaramillo, R. Gomperts, R. E. Stratmann, O. Yazyev, A. J. Austin, R. Cammi, C. Pomelli, J. W. Ochterski, P. Y. Ayala, K. Morokuma, G. A. Voth, P. Salvador, J. J. Dannenberg, V. G. Zakrzewski, S. Dapprich, A. D. Daniels, M. C. Strain, O. Farkas, D. K. Malick, A. D. Rabuck, K. Raghavachari, J. B. Foresman, J. V. Ortiz, Q. Cui, A. G. Baboul, S. Clifford, J. Cioslowski, B. B. Stefanov, G. Liu, A. Liashenko, P. Piskorz, I. Komaromi, R. L. Martin, D. J. Fox, T. Keith, M. A. Al-Latham, C. Y. Peng, A. Nanayakkara, M. Challacombe, P. M. W. Gill, B. Johnson, W. Chen, M. W. Wong, C. Gonzalez, and J. A. Pople, *Gaussian 03*, Revision D.02; Gaussian, Inc., Wallingford, CT, 2004.
- A. P. Scott and L. Radom, *J. Phys. Chem.*, 1996, **100**, 16502.
- A. D. Becke, *J. Chem. Phys.*, 1993, **98**, 5648–5652; C. Lee, W. Yang and R. G. Parr, *Phys. Rev. B: Condens. Matter*, 1988, **37**, 785.
- C. Adamo and V. Barone, *J. Chem. Phys.*, 1999, **110**, 6158.
- P. C. Hariharan and J. A. Pople, *Theor. Chim. Acta*, 1973, **28**, 213.
- T. Clark, J. Chandrasekhar and P. v. R. Schleyer, *J. Comput. Chem.*, 1983, **4**, 294.

- 21 J. W. Gauld, L. A. Eriksson and L. Radom, *J. Phys. Chem. A*, 1997, **101**, 1352.
- 22 N. Rega, M. Cossi and V. Barone, *J. Chem. Phys.*, 1996, **105**, 11060.
- 23 L. Hermosilla, P. Calle, J. M. Garcia de la Vega and C. Sieiro, *J. Phys. Chem. A*, 2005, **109**, 1114–1124; V. Barone, P. Cimino and E. Stendardo, *J. Chem. Theory Comput.*, 2008, **4**, 751.
- 24 G. Brigati, M. Lucarini, V. Mugnaini and G. F. Pedulli, *J. Org. Chem.*, 2002, **67**, 4828.
- 25 R. Amorati, M. G. Fumo, S. Menichetti, V. Mugnaini and G. F. Pedulli, *J. Org. Chem.*, 2006, **71**, 6325.
- 26 M. H. Abraham, P. L. Grellier, D. V. Prior, P. P. Duce, J. J. Morris and P. J. Taylor, *J. Chem. Soc., Perkin Trans. 2*, 1989, 699.
- 27 P. Mulder, H. G. Korth, D. A. Pratt, G. A. DiLabio, L. Valgimigli, G. F. Pedulli and K. U. Ingold, *J. Phys. Chem. A*, 2005, **109**, 2647.
- 28 M. I. de Heer, H. G. Korth and P. Mulder, *J. Org. Chem.*, 1999, **64**, 6969.
- 29 M. H. Abraham, P. L. Grellier, D. V. Prior, P. P. Duce, J. J. Morris and P. J. Taylor, *J. Chem. Soc., Perkin Trans. 2*, 1990, 521.
- 30 M. Foti, K. U. Ingold and J. Lusztyk, *J. Am. Chem. Soc.*, 1994, **116**, 9440.